

## Plasmon-enhanced photocurrent monitoring of the interaction between porphyrin covalently bonded to graphene oxide and adenosine nucleotides†

Cite this: *RSC Advances*, 2013, 3, 3503

Received 19th November 2012,

Accepted 10th January 2013

DOI: 10.1039/c3ra22935a

[www.rsc.org/advances](http://www.rsc.org/advances)

Cong Kong, Gan Zhang, Yang Li,\* Da-Wei Li and Yi-Tao Long\*

**Porphyrin covalently bonded to graphene oxide (Por-GO) was used as a photoactive unit, and resulted in an enhanced photoresponse, when in combination with gold nanoparticles (GNP) as a light harvesting unit, due to its plasmon resonance absorption effect. Photocurrent monitoring of the interaction between the surface-modified Por-GO with adenosine compounds was demonstrated.**

Nucleotides are composed of a nucleobase, a five-carbon sugar, and one to three phosphate groups.<sup>1</sup> When linked together by enzymes as a long, chain-like polynucleotide with a defined sequence, nucleotides make up the structural units ribonucleic acids (RNA) and deoxyribonucleic acids (DNA). The sequences of the nucleotide units along polynucleotide chains code for proteins and enzymes, as well as determining the genetic structure of life, playing important roles in storage, transfer and expression of genetic information.<sup>2,3</sup> Meanwhile, nucleotides perform other crucial functions in biological metabolic processes, such as cellular energy transportation and transformation, regulation of enzymes and cell signaling.<sup>4–6</sup>

The interactions between nucleotides and porphyrins have been studied and recently confirmed.<sup>7</sup> Investigation methods include NMR,<sup>8</sup> UV-vis,<sup>9,10</sup> circular dichroism<sup>11</sup> and linear dichroism<sup>12</sup> spectroscopy, among others. Several detection methods have been developed based on their interactions.<sup>13</sup> Porphyrin could be explored for possible applications within the therapies of cancer, porphyria, hematologic diseases and jaundice.<sup>14</sup> Due to their broad pronounced light absorption and preferable photoelectric activity, porphyrin derivatives are a favorable photoactive agent for various applications, such as solar energy conversion,<sup>15–18</sup> medical imaging,<sup>19</sup> photo therapy,<sup>20</sup> photo catalysis and sensing.<sup>21–23</sup> They are currently undergoing extensive investigation based on their excellent photocurrent activity.<sup>24,25</sup> Targeted drug delivery could be

achieved using various anticancer drugs linking to the porphyrin ring, due to its tendency to aggregate around the cancer cell, which intensifies the drug's pharmacological effects.<sup>26</sup> Studying the interaction between porphyrin derivatives and nucleotides is practically important in terms of examining, monitoring and creating new medical applications.<sup>27</sup>

Photocurrent measurements could feasibly be an analytical tool of low cost and high sensitivity due to the plentiful availability of substrates, repeatable use and elimination of undesired background signals by light excitation and current detection.<sup>13</sup> Nowadays, researchers in this field continue to be devoted to new materials and assembly of photosensitizers for more a efficient conversion of light into electricity and rapid photoresponse.<sup>28–30</sup> Graphene has recently attracted great attention due to its unique electronic properties, high transparency,<sup>31,32</sup> flexible structure, and large theoretical specific surface area,<sup>33</sup> holding much promise for various applications, such as making “paper-like” materials, batteries, hydrogen storage media, gas sensors and even an ultrafast photodetector.<sup>34–36</sup> Graphene oxide could efficiently separate and transfer photoinduced carriers from photoactive materials, making it a potential candidate for the generation of enhanced photoinduced electron separation on photosensitizers, and further increasing its photoresponse, which offers new opportunities to develop nanocomposites with unusual optoelectric properties.<sup>34</sup> Small gold or silver nanocrystals are plasmonic resonant nanoparticles that efficiently and strongly scatter light due to their collective oscillation of conducting electrons, from which a powerful tool for chemical and biological sensing experiments has been developed.<sup>37</sup> Up to now, several plasmon-related optical processes have been found and further explored for extensive applications.<sup>38–42</sup>

In our experiment, to monitor the interaction between porphyrin derivatives and nucleotides, we synthesized a porphyrin with covalently bonded graphene oxide, and further coated it on an indium tin oxide conductive (ITO) surface with Nafion. The established photoresponsive surface would generate a sensitive photocurrent in the presence of gold nanoparticles, which broaden and increase the photoabsorption efficiency on the functionalized surface, resulting in the enhanced photocurrent.

State Key Laboratory of Bioreactor Engineering & Department of Chemistry, East China University of Science and Technology, Shanghai, 200237, P. R. China.

E-mail: [ytlong@ecust.edu.cn](mailto:ytlong@ecust.edu.cn)

† Electronic supplementary information (ESI) available: Experimental details, synthesis of Por-GO and gold nanoparticles, characterization and more results. See DOI: 10.1039/c3ra22935a

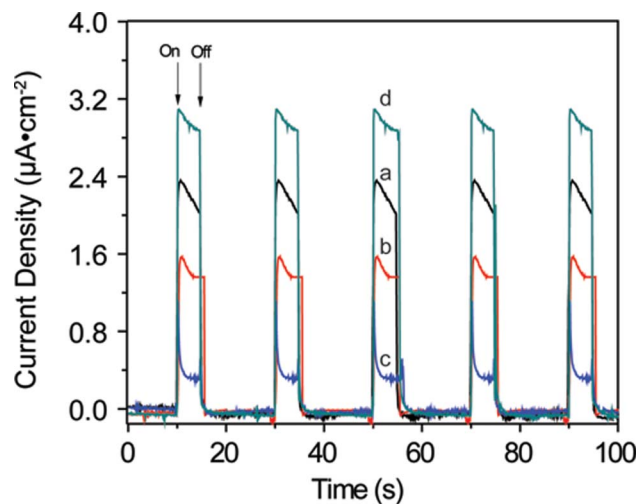


**Fig. 1** The photocurrent response of Por-GO-GNP (a), GNP-MV (b), Por-GO-MV (c), Por-GO-GNP-MV and (d) functionalized electrode, in a PBS 8.0 (phosphate buffered saline) solution containing 50 μM TEOA upon white light irradiation. "On" represents the electrode under light irradiation, while "Off" means the light was turned off.

Different photocurrent responses could be obtained depending on the interaction between the surface porphyrin groups and the nucleotides in solution. Compared with the traditional method, the photocurrent method allows real time and fast response processes with a low background signal. In addition, the developed system could be explored for applications in photo-voltaic cells. As a result, we achieved an enhanced photocurrent in our experiment and demonstrated its capacity to monitor the interaction.

To demonstrate the enhanced effect of each component on the photoresponse of the functionalized ITO electrodes, we examined the photoresponse of the Por-GO-GNP-MV (MV: methyl viologen) functionalized ITO electrode compared with the control electrode in the absence of each effective component, respectively. As shown in Fig. 1, the Por-GO-GNP-MV functionalized electrode gives the strongest photocurrent response compared to the control electrode. As the core component on the surface of this functional electrode, the GO would effectively extend the electron relay on the charge separated porphyrin, and further delay the charge recombination for its high electron conductivity and storage ability.<sup>43</sup> As a result, the photocurrent density of this electrode was 2 times higher than that of the control electrode without Por-GO. The surface plasmon resonance absorption allows GNP to act as an antenna to enhance the light absorption of porphyrin, and further increase the photocurrent of the functionalized electrode,<sup>44</sup> and so it can be seen that GNP plays an important role in enhancing the plasmon resonance. Consequently, we observed that the photocurrent density of the electrode is 6 times larger than that of the control without GNP. MV<sup>2+</sup> (methyl viologen dication) is regarded as an efficient electron acceptor and mediator, which has been widely used in the preparation of porphyrin-based photosensitive devices for catalysts and biosensors.<sup>45</sup> The photocurrent density on the as functionalized electrode

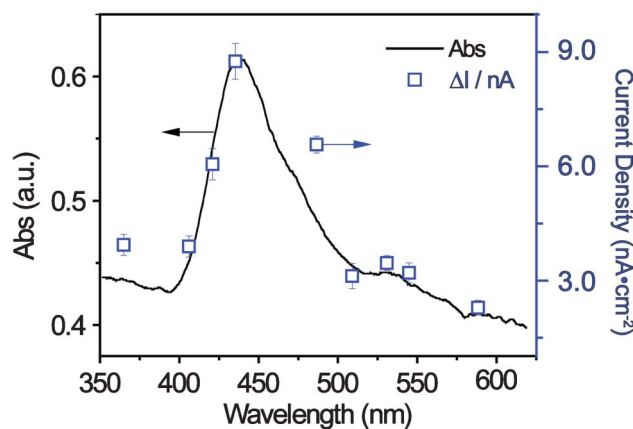
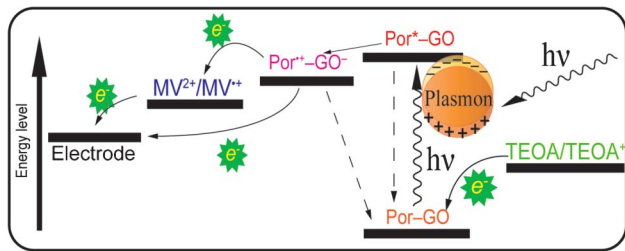


**Fig. 2** UV-vis absorption spectrum of Por-GO composites (black line). The photocurrent response of the Por-GO-GNP-MV functionalized electrode to the monochrome light of different wavelengths in PBS 8.0 solution containing 50 μM TEOA (blue square). Light filters were used to obtain different monochromatic light.

was 1.2 times higher than that of the control electrode without MV<sup>2+</sup>. Moreover, triethanolamine (TEOA) as a sacrificial electron donor in the solution, leads to a much higher and efficient photocurrent collection with the ITO electrode, as shown in Fig. S4†. In our experiment, we introduced Nafion for its role in binding the effective components, protecting the photoactive material from degrading under light and stabilizing the surface by forming a strong membrane. As a result, our design enhanced the photocurrent response on the ITO electrode.

Due to the presence of several components, such as GNP, MV<sup>2+</sup> and Por-GO, on the functionalized electrode, the photoexcited electron source as a main unit to generate photocurrent should be clarified. We used light at different wavelengths to irradiate the electrode and then compared it to the UV-vis absorption curve of Por-GO in PBS 8.0 solution. Fig. 2 shows the UV-vis spectra of Por-GO composites, as well as the photocurrent density of the modified ITO electrode irradiated by a light source with varying wavelength under working conditions. When irradiated by light at a wavelength of 425–450 nm, where the Por-GO composites showed the strongest absorption in the UV-vis spectrum, photocurrents with the maximum density could be observed, in addition to higher photocurrent responses obtained at the wavelength where surface plasmon resonance absorbance occurred on GNP. However, a photocurrent of low intensity was observed at the wavelength where both the Por-GO and GNP have weak absorption. The coincidence between absorption and photocurrent proved that the Por-GO sheets and GNP acted as the dominant photosensitive species on the functionalized electrode.<sup>49</sup>

Based on the different role of each component in the photocurrent generation process, we proposed the possible mechanism of electron transfer. Briefly, electrons at the ground state are excited from the porphyrin under irradiation to their excited state. Some of the electrons are transferred directly to GO, the other portion would transfer onto MV to form methyl viologen radicals (MV<sup>•+</sup>), which provide an electron relay. Subsequently,



**Scheme 1** A schematic illustration of electron transfer during the photocurrent generation on the functionalized electrode.

TEOA gives electrons to porphyrin to refill the deficient electron on the ground state. Then, the separated electron on the  $MV^+$  and GO would transfer into the ITO electrode under a given applied potential, resulting in stable and efficient photocurrent generation. The photoinduced electron-transfer process that has occurred on the functionalized ITO electrode is depicted in Scheme 1.

After the construction of the functionalized ITO electrode, its photocurrent response to adenosine nucleotides including adenosine (Ade), adenosine monophosphate (AMP), adenosine diphosphate (ADP) and adenosine triphosphate (ATP), was examined in solution to monitor the surface-modified porphyrin interactions. Fig. 3 shows the photocurrent change profile before and after individual additions of these nucleotides at a constant concentration of  $3\ \mu\text{M}$  in the supporting electrolyte solution. It could be found that the addition of adenosine nucleotides in the solution decreased the photocurrent response of the functionalized ITO electrode in the background solution.

We define  $\Delta I$  as the difference between the current of the electrode before and after light irradiation. The photocurrent response of the functionalized electrode to these nucleotides was calculated as the ratio of the photocurrent discrepancy to the background photocurrent, before ( $\Delta I_{\text{back}}$ ) and after ( $\Delta I_{\text{resp}}$ ) the

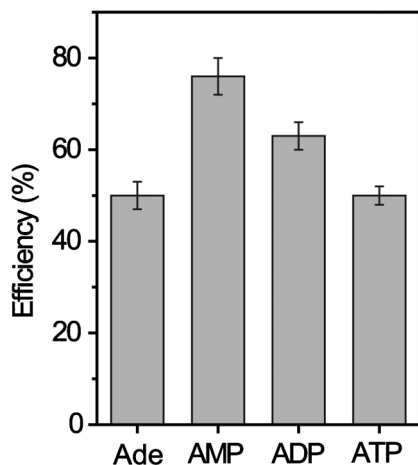
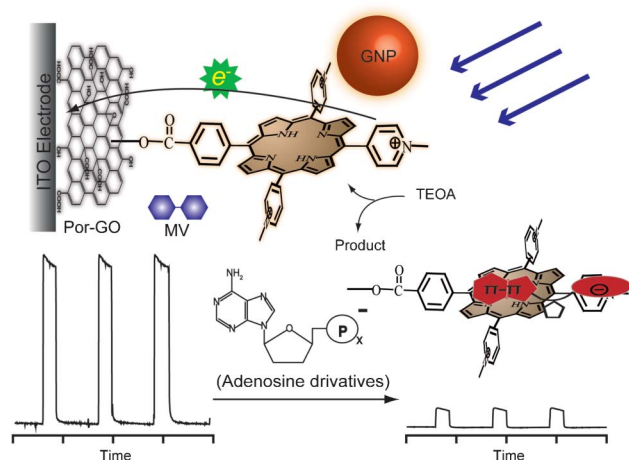


**Fig. 3** Quenching of the photocurrent by adding different nucleotides (adenosine, AMP, ADP and ATP) at a concentration of  $3\ \mu\text{M}$  (PBS 8.0, 0.2 M. TEOA,  $50\ \mu\text{M}$ ). The percentages of reduction compared with original photocurrent responses are shown.

addition of a nucleotide. Among the four nucleotides being studied in our research, AMP was found to induce the strongest drop of photocurrent density with *ca.* 76% reduction compared with original background intensity. Their interactions with the modified porphyrin surface are rated as  $\text{AMP} > \text{ADP} > \text{ATP} > \text{Ade}$ , by their photocurrent response profile on the functionalized surface.

The interaction of the functionalized ITO electrode with adenosine nucleotides may be attributed to the  $\pi$ - $\pi$  stacking interaction, electrostatic interaction or a steric hindrance effect. The  $\pi$ - $\pi$  stacking effect and interaction between the porphyrin and adenosine nucleotide have been studied through absorption spectroscopy, circular dichroism, linear dichroism and NMR spectra in previous studies.<sup>8</sup> In our research, the possible  $\pi$ - $\pi$  stacking effect between them is proposed to inhibit the photo-induced electron transfer from the excited porphyrin to adjacent GO or  $MV^{2+}$  acceptors.<sup>50</sup> Furthermore, the  $\pi$ - $\pi$  complexation effect may block the contact of sacrificial electron donors (TEOA) to the porphyrin derivatives. Besides, the electron static interaction between the negatively charged nucleotide and positively charged porphyrin could also facilitate their complexation.<sup>10</sup> As a result, their interaction may vary with the structure of nucleotide, which leads to different binding abilities to porphyrin by the different  $\pi$ - $\pi$  stacking and electrostatic interactions. Moreover, the steric hindrance effect originating from the nucleotide structure could bring about different binding abilities between the porphyrin and nucleotides. Although ADP and ATP contain more negative charge than AMP, a stronger steric hindrance effect between them and the porphyrin may block the stack process, leading to a less facile interaction. Adenosine showed the least interaction with the porphyrin due to its lower electrostatic attraction compared with adenosine phosphate derivatives. In the tested nucleotides, as AMP has shown the greater stacking ability, electrostatic interaction and less steric hindrance, which benefits its binding to the porphyrin, the most sensitive photocurrent drop was observed on the prepared functionalized ITO electrode. The photocurrent generation and interaction profile of the adenosine nucleotide with the surface are illustrated in Scheme 2.

Real time monitoring of the interaction between adenosine nucleotides and surface porphyrin derivatives was demonstrated as the photocurrent generation on the Por-GO-GNP-MV functionalized ITO electrode varies in the presence of adenosine nucleotides. As different types of nucleotide were added into the electrolyte solution, the photocurrent response changed on the functionalized electrode, showing the different interaction abilities between the adenosine nucleotides and porphyrin derivatives on the surface. Fig. 4 shows the photocurrent monitoring of the interaction of adenosine derivatives with the surface porphyrin derivatives, where different concentrations of adenosine nucleotides were added to the solution, resulting in the photocurrent response changing immediately. The fact that addition of different kinds of adenosine nucleotides leads to a different photocurrent response, proving the possibility of using the functionalized electrode to monitor the interaction process. The process further proved the possibility of photocurrent monitoring of the interac-



**Scheme 2** An illustration of photocurrent generation on the Por-GO-GNP-MV functionalized surface and the photocurrent decrease induced by its interaction with nucleotide.

tion between the surface functionalized molecules with the one in solution.

Overall, we synthesized covalently bonded porphyrin GO composites and further explored their photoresponse properties by functionalizing them on the surface of electrodes with different enhancing components. To improve the sensitivity of the functionalized ITO electrode, methyl viologen was used as an electron acceptor to reinforce its electron transfer, and gold nanoparticles were used to increase the light absorption for its plasmon resonance effect. We enhanced the photocurrent of the functionalized interface *via* incorporation of GNPs and MV<sup>2+</sup> on the Nafion film. Moreover, a highly efficient Por-GO-GNP-MV functionalized ITO electrode as a sensor for real time monitoring of their interactions with adenosine nucleotides in aqueous

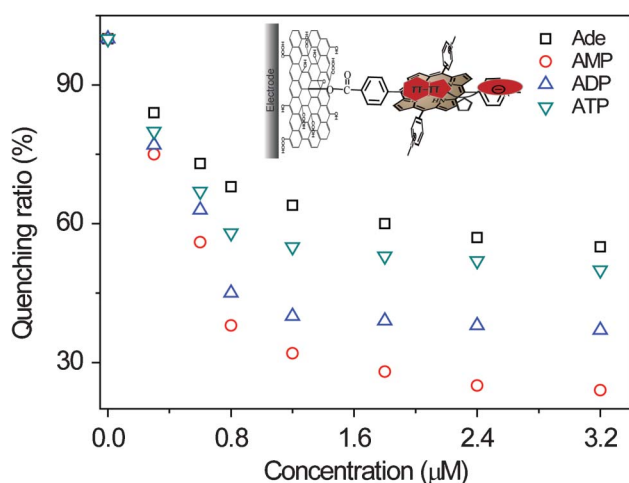


**Fig. 4** Photocurrent monitoring of the surface solution interaction in the presence of different concentrations of Ade (square), AMP (circle), ADP (triangle) and ATP (inverted triangle). The insert illustrates the interaction between adenosine derivatives with porphyrin based on the  $\pi$ - $\pi$  stacking, electrostatic interaction or a steric hindrance effect.

solution was constructed using Por-GO composites as a sensing agent and an ITO electrode as a modification substrate. The functionalized electrode showed different photocurrent responses depending on the presence of different nucleotides, showing its promising capacity in monitoring the interaction of nucleotides in solution with the functionalized surface. This method further demonstrated, as a proof-of-concept, the possibility of photocurrent monitoring of interface interactions. Further exploration of surfaces modified with photoactive substances to investigate the surface-to-solution interactions are expected.

The authors would like to thank the Specialized Research Fund for the Doctoral Program of Higher Education (20100074120017), the 973 program (2013CB733700), the Shanghai Municipal Natural Science Foundation (11ZR1408900), National Natural Science Foundation of China (21105028), the Major Research Plan of National Natural Science Foundation of China (91027035) and the Fundamental Research Funds for the Central Universities (WK1013002, WK1214021, WB1113005).

## Notes and references

- 1 R. Dahm, *Hum. Genet.*, 2008, **122**, 565–581.
- 2 E. S. Lander, L. M. Linton and B. Birren *et al.*, *Nature*, 2001, 409, 860–921.
- 3 L. C. Kühn, A. McClelland and F. H. Ruddle, *Cell*, 1984, **37**, 95–103.
- 4 P. P. Dzeja and A. Terzic, *J. Exp. Biol.*, 2003, **206**, 2039–2047.
- 5 M. Erecińska and D. F. Wilson, *J. Membr. Biol.*, 1982, **70**, 1–14.
- 6 A. Pradet and P. Raymond, *Annu. Rev. Plant Physiol.*, 1983, **34**, 199–224.
- 7 P. Kubat, K. Lang, P. Anzenbacher Jr, K. Jursikova, V. Kral and B. Ehrenberg, *J. Chem. Soc., Perkin Trans. 1*, 2000, 933–941.
- 8 R. F. Pasternack, E. J. Gibbs, A. Antebi, S. Bassner, L. De Poy, D. H. Turner, A. Williams, F. Laplace and M. H. Lansard, *J. Am. Chem. Soc.*, 1985, **107**, 8179–8186.
- 9 M. Sirish and H.-J. Schneider, *Chem. Commun.*, 2000, 23–24.
- 10 M. Sirish and H.-J. Schneider, *J. Am. Chem. Soc.*, 2000, **122**, 5881–5882.
- 11 J. Nový and M. Urbanová, *Biopolymers*, 2007, **85**, 349–358.
- 12 M.-J. Lee, B. Jin, H. M. Lee, M. J. Jung, S. K. Kim and J.-M. Kim, *Bull. Korean Chem. Soc.*, 2008, **29**, 1533–1538.
- 13 A. Ikeda, M. Nakasu, S. Ogasawara, H. Nakanishi, M. Nakamura and J.-i. Kikuchi, *Org. Lett.*, 2009, **11**, 1163–1166.
- 14 S. Sun, D. Wu, Q. Wei, Y. Han, X. Chen, Y. Shen, P. Zhu and B. Du, *J. Fluoresc.*, 2009, **19**, 809–815.
- 15 V. Chukharev, T. Vuorinen, A. Efimov, N. V. Tkachenko, M. Kimura, S. Fukuzumi, H. Imahori and H. Lemmetyinen, *Langmuir*, 2005, **21**, 6385–6391.
- 16 T. Akiyama, K. Aiba, K. Hoashi, M. Wang, K. Sugawa and S. Yamada, *Chem. Commun.*, 2010, **46**, 306–308.
- 17 T. Yui, Y. Kobayashi, Y. Yamada, K. Yano, Y. Fukushima, T. Torimoto and K. Takagi, *ACS Appl. Mater. Interfaces*, 2011, **3**, 931–935.
- 18 P. N. Ciesielski, C. J. Faulkner, M. T. Irwin, J. M. Gregory, N. H. Tol, D. E. Cliffel and G. K. Jennings, *Adv. Funct. Mater.*, 2010, **20**, 4048–4054.
- 19 X. Zhang, Z. X. Liu, L. Ma, M. Hossu and W. Chen, *Nanotechnology*, 2011, **22**, DOI: 10.1088/0957-4484/22/19/195501.



- 20 M. Ethirajan, Y. Chen, P. Joshi and R. K. Pandey, *Chem. Soc. Rev.*, 2011, **40**, 340–362.
- 21 C. X. Guo, Y. Lei and C. M. Li, *Electroanalysis*, 2011, **23**, 885–893.
- 22 L. Lvova, R. Paolesse, C. Di Natale and A. Damico, *Sens. Actuators, B*, 2006, **118**, 439–447.
- 23 B. Johnson-White, M. Zeinali, K. M. Shaffer, C. H. Patterson Jr, P. T. Charles and M. A. Markowitz, *Biosens. Bioelectron.*, 2007, **22**, 1154–1162.
- 24 H. Hosono and M. Kaneko, *J. Chem. Soc., Faraday Trans.*, 1997, **93**, 1313–1319.
- 25 T. Hasobe, H. Imahori, T. Sato, K. Ohkubo and S. Fukuzumi, *Nano Lett.*, 2003, **3**, 409–412.
- 26 X. Chen, L. Hui, D. A. Foster and C. M. Drain, *Biochemistry*, 2004, **43**, 10918–10929.
- 27 M. Nowostawska, S. A. Corr, S. J. Byrne, J. Conroy, Y. Volkov and Y. K. Gun'ko, *J. Nanobiotechnology*, 2011, **9**, DOI: 10.1186/1477-3155-9-13.
- 28 M. Miyachi, Y. Yamanoi, Y. Shibata, H. Matsumoto, K. Nakazato, M. Konno, K. Ito, Y. Inoue and H. Nishihara, *Chem. Commun.*, 2010, **46**, 2557–2559.
- 29 M. De Crescenzi, F. Tombolini, M. Scarselli, S. D. Gobbo, E. Speiser, P. Castrucci, M. Diociaiuti, S. Casciardi, E. Gatto and M. Venanzi, *Surf. Sci.*, 2007, **601**, 2810–2813.
- 30 R. Freeman, R. Gill, M. Beissenhirtz and I. Willner, *Photochem. Photobiol. Sci.*, 2007, **6**, 416–422.
- 31 C. Chen, W. Cai, M. Long, B. Zhou, Y. Wu, D. Wu and Y. Feng, *ACS Nano*, 2011, **4**, 6425–6432.
- 32 R. R. Nair, P. Blake, A. N. Grigorenko, K. S. Novoselov, T. J. Booth, T. Stauber, N. M. R. Peres and A. K. Geim, *Science*, 2008, **320**, 1308.
- 33 S. Sun, L. Gao and Y. Liu, *Appl. Phys. Lett.*, 2010, **96**, 083113–083113.
- 34 Y. Lin, K. Zhang, W. Chen, Y. Liu, Z. Geng, J. Zeng, N. Pan, L. Yan, X. Wang and J. G. Hou, *ACS Nano*, 2010, **4**, 3033–3038.
- 35 F. Xia, T. Mueller, Y.-m. Lin, A. Valdes-Garcia and P. Avouris, *Nat. Nanotechnol.*, 2009, **4**, 839–843.
- 36 D. A. Dikin, S. Stankovich, E. J. Zimney, R. D. Piner, G. H. B. Dommett, G. Evmenenko, S. T. Nguyen and R. S. Ruoff, *Nature*, 2007, **448**, 457–460.
- 37 Y. Li, C. Jing, L. Zhang and Y. T. Long, *Chem. Soc. Rev.*, 2012, **41**, 632–642.
- 38 G. Hong, S. M. Tabakman, K. Welsher, H. Wang, X. Wang and H. Dai, *J. Am. Chem. Soc.*, 2010, **132**, 15920–15923.
- 39 A. R. Guerrero and R. F. Aroca, *Angew. Chem., Int. Ed.*, 2011, **50**, 665–668.
- 40 S. Cataldo, J. Zhao, F. Neubrech, B. Frank, C. Zhang, P. V. Braun and H. Giessen, *ACS Nano*, 2011, **6**, 979–985.
- 41 F. Le, D. W. Brandl, Y. A. Urzhumov, H. Wang, J. Kundu, N. J. Halas, J. Aizpurua and P. Nordlander, *ACS Nano*, 2008, **2**, 707–718.
- 42 K. A. Willets and R. P. Van Duyne, *Annu. Rev. Phys. Chem.*, 2007, **58**, 267–297.
- 43 Y. Xu, Z. Liu, X. Zhang, Y. Wang, J. Tian, Y. Huang, Y. Ma, X. Zhang and Y. Chen, *Adv. Mater.*, 2009, **21**, 1275–1279.
- 44 I. Kim, S. L. Bender, J. Hranisavljevic, L. M. Utschig, L. Huang, G. P. Wiederrecht and D. M. Tiede, *Nano Lett.*, 2011, **11**, 3091–3098.
- 45 S. Cherian and C. C. Wamser, *J. Phys. Chem. B*, 2000, **104**, 3624–3629.
- 46 Y. Li, Y. Liu, N. Wang, Y. Li, H. Liu, F. Lu, J. Zhuang and D. Zhu, *Carbon*, 2005, **43**, 1968–1975.
- 47 A. J. Esswein and D. G. Nocera, *Chem. Rev.*, 2007, **107**, 4022–4047.
- 48 H. Yamada, H. Imahori, Y. Nishimura, I. Yamazaki, T. K. Ahn, S. K. Kim, D. Kim and S. Fukuzumi, *J. Am. Chem. Soc.*, 2003, **125**, 9129–9139.
- 49 Y.-J. Cho, T. K. Ahn, H. Song, K. S. Kim, C. Y. Lee, W. S. Seo, K. Lee, S. K. Kim, D. Kim and J. T. Park, *J. Am. Chem. Soc.*, 2005, **127**, 2380–2381.
- 50 M. J. Lee, B. Jin, H. M. Lee, M. J. Jung, S. K. Kim and J. M. Kim, *Bull. Korean Chem. Soc.*, 2008, **29**, 1533–1538.